Tumor and Stem Cell Biology

Cancer Research

Loss of Function of the Tumor Suppressor DKC1 Perturbs p27 Translation Control and Contributes to Pituitary Tumorigenesis

Cristian Bellodi[1], Olya Krasnykh[1], Nikesha Haynes[1], Marily Theodoropoulou[2], Guang Peng[1], Lorenzo Montanaro[3], and Davide Ruggero[1]

Abstract

Mutations in *DKC1*, encoding for dyskerin, a pseudouridine synthase that modifies rRNA and regulates telomerase activity, are associated with ribosomal dysfunction and increased cancer susceptibility in the human syndrome, X-linked dyskeratosis congenita (X-DC). In a mouse model for X-DC, impairments in DKC1 function affected the translation of specific mRNAs harboring internal ribosomal entry site (IRES) elements, including the tumor suppressor, p27. However, how this translational deregulation contributes to tumor initiation and progression remains poorly understood. Here, we report that impairment in p27 IRES-mediated translation due to decreased levels of DKC1 activity markedly increases spontaneous pituitary tumorigenesis in p27 heterozygous mice. Using a new bioluminescent mouse model, we monitored p27 translation *in vivo* and show that p27 IRES-mediated translation is reduced in the pituitary of DKC1 hypomorphic mice ($DKC1^{m}$). Furthermore, we show that DKC1 has a critical role in regulating the assembly of the 48S translational preinitiation complex mediated by the p27 IRES element. An analysis of human tumors identified a novel mutation of *DKC1* ($DKC1^{S485G}$) in a human pituitary adenoma. We show that this specific amino acid substitution significantly alters DKC1 stability/pseudouridylation activity, and this correlates with reductions in p27 protein levels. Furthermore, $DKC1^{S485G}$ mutation does not alter telomerase RNA levels. Altogether, these findings show that genetic alterations in DKC1 could contribute to tumorigenesis associated with somatic cancers and establish a critical role for DKC1 in tumor suppression, at least in part, through translational control of p27. *Cancer Res; 70(14); 6026–35. ©2010 AACR.*

Introduction

Inherited mutations in the X-linked *DKC1* gene, which encodes for dyskerin (a pseudouridine synthase that modifies rRNA), are associated with the pathogenesis of a severe form of dyskeratosis congenita (X-DC) characterized by increased susceptibility to cancer (1). In addition, DKC1 expression is found to be deregulated in many human cancers, including a subset of prostate cancers, B-chronic lymphocytic leukemia, and breast carcinomas (2–4). Therefore, somatic mutations in ribosome components, such as DKC1, may have broad implications for tumorigenesis. DKC1 functions within ribonucleoprotein complexes in combination with the box H/ACA small nucleolar RNAs to catalyze the isomerization of specific uridines (U) into pseudouridines (ψ) on rRNA, a process known as pseudouridylation. Besides its role as a pseudouridine synthase, DKC1 is also implicated in telomere maintenance and mRNA splicing through physical association with the RNA component of the human telomerase (TERC) and small Cajal body RNAs, respectively (5). We have previously generated DKC1 mutant mice ($DKC1^{m}$) that faithfully recapitulated all the pathologic features of X-DC, including an increase in cancer susceptibility (6). Importantly, $DKC1^{m}$ mice display reductions in rRNA modifications prior to the onset of disease when the telomere's length is unperturbed (6). An outstanding question that remains to be answered is the role of DKC1 as a tumor suppressor in somatic cancers. Indeed, to date, somatic mutations in the *DKC1* gene have not been identified.

Internal ribosomal entry site (IRES)–dependent translation is a finely tuned mechanism that regulates the expression of specific mRNAs during distinct cellular processes such as apoptosis, quiescence, and differentiation (7). Deregulation of IRES-mediated translation has been associated with tumor initiation and progression (8, 9). We have previously shown that the loss of function in DKC1 results in a defect in the translation of specific mRNAs that all harbor IRES elements

Authors' Affiliations: [1]School of Medicine and Department of Urology, Helen Diller Family Comprehensive Center, University of California, San Francisco, San Francisco, California; [2]Max Planck Institute of Psychiatry, Munich, Germany; and [3]Department of Experimental Pathology, University of Bologna, Bologna, Italy

Note: Supplementary data for this article are available at Cancer Research Online (http://cancerres.aacrjournals.org/).

Corresponding Author: Davide Ruggero, Helen Diller Family Comprehensive Center, University of California, San Francisco, 1450 3rd Street, Room 386, MC 3110, San Francisco, CA 94158. Phone: 415-514-9755; Fax: 415-514-4826; E-mail: davide.ruggero@ucsf.edu.

doi: 10.1158/0008-5472.CAN-09-4730

in their 5′-untranslated region, including the cell cycle regulator and tumor suppressor gene, p27. These translational defects present in DKC1^{m} cells are also recapitulated in X-DC patient cells (10).

Here, we genetically show a critical function for p27 translational control in pituitary tumor suppression that is mediated through dyskerin activity. Several cell cycle regulator genes including *p27* are lost or aberrantly expressed in pituitary adenomas (11). For example, loss of one copy of the retinoblastoma (Rb) gene is almost invariably associated with the formation of spontaneous pituitary cancers in both mice and humans (12–14). High levels of the gene encoding the pituitary tumor-transforming protein (PTTG), important for the mitotic checkpoint, are observed in pituitary adenomas, and also correlate with tumor invasiveness and recurrence (15, 16). Importantly, the expression of p27 is often reduced in pituitary and other human cancers without mutations in the gene locus (17). p27$^{-/-}$ mice develop spontaneous pituitary tumors (18). In human pituitary tumors, loss of function of p27 occurs at the posttranscription level and without increases in SKP2 expression, which regulates p27 protein stability (19). This suggests that other mechanisms might be involved in controlling p27 expression, which may be important for tumor suppression (19). Indeed, the *p27* gene is tightly regulated posttranscriptionally (20–22). For example, translation of p27 is maximal in quiescence and early G_1 phase of the cell cycle through an IRES element positioned in its 5′-untranslated region (23–25).

Using a new bioluminescent mouse model to directly monitor p27 IRES-dependent translation *in vivo*, we show that p27 IRES-mediated translation occurs in the pituitary. Moreover, we show that p27 IRES-mediated translation is dramatically reduced in the pituitary of DKC1^{m} animals. We then delineate the molecular mechanism by which reductions in rRNA pseudouridylation impinge on a critical step of p27 IRES-mediated translation control. In addition, we functionally show that DKC1^{m};p27$^{+/-}$ mice develop a similar spectrum of pituitary malignancies as p27$^{-/-}$ mice. Finally, we report the first mutation of the *DKC1* gene in a patient with pituitary adenoma that results in a drastic reduction of DKC1 expression and pseudouridylation activity which correlates with significant decrease of p27 protein levels. These findings delineate the critical role of DKC1 as a tumor suppressor gene in controlling gene expression at the translational level as a barrier against tumor development.

Materials and Methods

Generation of p27-IRES^{T} mice and luciferase assay

The p27 IRES^{T} mice were generated using a pCMV-Myc-RL-p27 IRES-FL construct. The p27 IRES element (10) was subcloned into pCR 2.1 (Invitrogen), digested with *Eco*RI, and inserted into a pRF plasmid. The RL-HCV IRES-FL was amplified, digested using *Bgl*II and *Kpn*I, and inserted into the pCMV-Myc expression vector. The resulting pCMV-Myc-RL-p27 IRES-FL was linearized using an *Alw*44I restriction enzyme and microinjected into mouse embryos that were then implanted into female recipient mice. Founder lines were generated, genotyped, and crossed with wild-type (WT) mice to verify germ line transmission. To confirm that there was no splicing of the transgenic p27 IRES^{T} dicistronic RNA, retro-transcriptase PCR (RT-PCR) was performed to amplify a 2.3-kb fragment spanning from the sequence upstream of the Renilla coding region (P1) up to the Firefly coding region (P2). A second RT-PCR was carried out using primers on the Renilla (P3) and Firefly (P2) sequences to amplify a 750-bp fragment containing the p27 IRES element. The following primers were used: P1, 5′-GCTAGCCACCATGACTTCGAAAG; P2, 5′-GATGTTCACCTCGATATGTGC; and P3, 5′-GTTTATTGAATCGGACCCAGG.

Determination of p27 IRES-mediated translation

Analysis of p27 IRES activity was performed using the Dual Luciferase kit (Promega) protocol with some modifications. Different organs from p27 IRES^{T} mice were surgically removed and immediately transferred to a suitable amount of passive lysis buffer (Promega). Subsequently, tissue lysates were subjected to one cycle of freeze-thawing and homogenized using a tissue pulverizer. Lysates were incubated on ice for 30 minutes, and an aliquot of 20 to 40 μL was used to measure the FLuc (IRES) and RLuc (cap) activities using a single tube luminometer Optocomp1 (MGM Instruments). The expression levels of the p27 IRES dicistronic mRNA, which were determined using quantitative PCR (QPCR), were used to normalize luciferase activities. Pituitary glands from p27 IRES^{T} and p27 IRES^{T};DKC1^{m} animals were surgically removed and immediately transferred in 50 μL of passive lysis buffer. The ratio between FLuc (IRES) and RLuc (cap) Fluc activity was measured as described above.

Histological analysis of the pituitary gland

The excised pituitary glands were immediately fixed in 10% buffered formalin. Fixed tissue specimens were subsequently transitioned into ethanol and embedded in paraffin blocks. Tissue blocks were cut into 5 mm thickness on a Leica microtome. Sections were dried onto glass slides, deparaffinized by incubation at 55°C, and with the use of xylene, rehydrated in descending grades of alcohol and stained using a standard H&E protocol.

Cloning of DKC1^{S485G} mutant

The DKC1^{S485G} mutant was generated using a site-directed mutagenesis kit (Stratagene) according to the instructions of the manufacturer. Human DKC1 cDNA was prepared from total mRNA isolated from HeLA cells, and was then FLAG-tagged and subcloned into pCDNA3.1 (Invitrogen). Primers for site-directed mutagenesis were forward, AGGCCAAAGCTGGTCTGGAGGGCGGGGCCGAGCCTGGAGATGG; and reverse, CCATCTCCAGGCTCGGCCCCGCCCTCCAGACCAGCTTTGGCCT. Mutagenesis was confirmed by direct sequencing of the plasmid.

Analysis of protein stability

The stability of DKC1^{S485G} mutant was analyzed as described (10), with some modifications. Briefly, HeLa cells were plated on a six-well plate at a density of 200,000

cells/well and transfected with expression vectors encoding for full-length WT DKC1 or DKC1^{S485G} along with a pEGFP to normalize transfection efficiency. Twenty-four hours later, cells were cultured in the presence of 50 μg/mL of cycloheximide (Sigma) and harvested at the indicated time points. Protein analysis was carried out using standard protocols. The following antibodies and dilutions were used: anti-FLAG (1:1,000; Sigma), anti–β-actin (1:5,000; Sigma), and anti-GFP (1:250; SCBT).

Analysis of 48S preinitiation complex

Analysis of the 48S preinitiation complex formation was performed as described (26). Briefly, the p27 IRES monocistronic plasmid was linearized, *in vitro* transcribed, and radiolabeled using a MAXIscript T7 kit (Ambion, AM1312) in the presence of 50 μCi of [α-^{32}P]UTP (NEN). Radiolabeled [^{32}P]p27 IRES RNA was incubated with cytoplasmic extracts prepared from serum-starved (0.1% serum) WT and DKC1^{m}. Cells were harvested and lysed in RLN lysis buffer [10 mmol/L Tris-HCl (pH 8.0), 140 mmol/L NaCl, 1.5 mmol/L $MgCl_2$, 20 units of RNasin, 0.25% NP40, 150 μg/mL cyclohexamide, and 20 mmol/L DTT]. Protein extracts were preincubated for 2 minutes at 30°C with the components necessary for translation initiation [1 mmol/L ATP, 10 mmol/L creatine phosphate, 1 mg/mL creatine phosphokinase, 0.02 mmol/L L-methionine, and 12.5 mmol/L HEPES-KOH (pH 7.3)] as well as the translation initiation inhibitor—4 mmol/L of GMP-PNP (G0635-5MG; Sigma), 0.3 mmol/L of cyclohexamide, and 0.25 mmol/L of spermidine. 48S translation initiation complexes were formed by incubating the mixtures with the [^{32}P]p27 IRES mRNA probe for 15 minutes at 30°C. Following incubation, the samples were run on 10% to 30% sucrose density gradients on a SW55 Beckman rotor at 55,000 rpm and 4°C for 2.5 hours. Gradients were then fractionated into 200 μL fractions; each was immersed into 1 mL of 30% scintillation fluid (Fisher, SX23-5) and counted on a Beckman scintillation counter. Counts per minute were plotted against the fraction number.

Patients

This study was approved by the Ethics Committee of the Max Planck Institute. Informed consent was received directly from patients or their relatives. Samples from 35 pituitary tumors and 2 normal human pituitary glands were obtained from autopsy cases without any evidence of endocrinologic disease, with postmortem delays of between 8 and 12 hours. The pituitary adenoma specimens analyzed in this study included 15 acromegaly-associated adenomas, 4 corticotrophinomas, and 16 nonfunctioning pituitary adenoma. Adenomas were diagnosed by clinical, radiological, and surgical findings. Adenomas as well as normal tissue samples were collected after surgical resection and immediately snap-frozen in liquid nitrogen. Samples were stored at −80°C before mRNA preparation. Specifically, normal tissue specimens were collected at autopsy and RNA quality was analyzed using a spectrophotometer and by gel electrophoresis. RNA preparations were considered pure when the absorbance ratio 260/280 nm was between 1.6 and 2.0, and no degradation was evident from the RNA gel.

Real-time quantitative PCR analysis of DKC1 and p27 mRNA levels from human samples

Total RNA was extracted from frozen samples using Trizol reagent (Invitrogen). For each sample, total RNA was reverse transcribed using the High-Capacity cDNA Archive Kit (Applied Biosystems) following the instructions of the manufacturer. Real-time PCR analysis of cDNA was performed using a Gene Amp 7000 Sequence Detection System (Applied Biosystems). Cycling conditions were the following: 50°C for 2 minutes, 95°C for 10 minutes, 40 cycles at 95°C for 15 seconds, and 60°C for 1 minute. Primers and fluorogenic probes for DKC1 (Hs00154737_m1), p27 (Hs00153277_m1), and human β-glucuronidase (4326320E) were purchased from Applied Biosystems. Telomerase RNA analysis was performed as described elsewhere (2). The following primers were used: TERC forward 5′-GGTGGTGGCCATTTTTTGTC-3′ and TERC reverse 5′-CTAGAATGAACGGTGGAAGGC-3′ and TERC TaqMan probe 5′-CGCGCTGTTTTTCTCGCTGACTTTC-3′. Samples were analyzed in triplicate and the relative amount of mRNA was determined using the −ΔΔCt methods.

p27 and DKC1 Western blot analysis from human samples

Normal and tumor specimens were treated by lysis buffer [KH_2PO_4 0.1 mol/L (pH 7.4), 1% Igepal CA 630; Sigma Chemical] at 4°C, homogenized, and centrifuged. Supernatants were used for Western blot analysis by standard protocols using anti-p27 and anti-DKC1 antibodies (clone DCS-72; MBL International and SCBT, H300).

Measure of rRNA pseudouridylation

Evaluation of rRNA pseudouridylation was carried out as previously described (2). Briefly, 40 μg of total RNA were electrophoresed on a 1.2% agarose-2.2 mol/L formaldehyde gel and 28S and 18S rRNA was purified from the gel using DNA ultrafree DA spin columns (Millipore Corporation). The 18S rRNA was treated with RNase T2 (Sigma-Aldrich) for 1 hour at 37°C in 10 mmol/L of ammonium acetate buffer (pH 5.5). The resulting nucleotides were then dephosphorylated using alkaline phosphatase (Fluka, Sigma-Aldrich) for 1 hour at 37°C after the addition of 0.4 vol. of 50 mmol/L Tris base and 0.1 vol. of $MgCl_2$ 10 mmol/L. The resulting nucleosides were then subjected to high-performance liquid chromatographic separation in a Beckman System Gold Programmable Solvent Module 126 equipped with a detector Module 166 set at 254 nm (Beckman-Coulter). The column was a reverse-phase μBondapak C_{18} (particle size 10 μm) purchased from Waters Associates. Mobile phase conditions were 0.1 mol/L phosphate buffer (pH 6)/methanol at 99:1 (v/v) for 12 minutes, 96:4 (v/v) for 13 minutes, and 85:15 (v/v) for 25 minutes. Pseudouridine and major nucleosides used as standards were purchased from Berry and Associates, Inc.

Results

Use of bioluminescent mice to monitor p27 IRES-dependent translation *in vivo* reveals robust translational control in the pituitary, which is reduced in the DKC1^{m} background

We have previously shown that translational control of *p27* gene expression is impaired in DKC1^{m} mice and X-DC patient cells (10). We therefore sought to directly monitor p27 IRES-dependent translation *in vivo*. To this end, we generated the first bioluminescent transgenic mouse model (p27 IRES^{T}) to monitor p27 IRES-dependent translation *in vivo*. P27 IRES^{T} mice harbor a dicistronic reporter gene controlled by the cytomegalovirus ubiquitous promoter. Specifically, the expression of the transgene led to the production of a dicistronic mRNA in which the first cistron (RLuc) is translated via cap-dependent translation, whereas the second cistron (FLuc) is translated under the control of the p27 IRES element (Fig. 1A). We ruled out the possibility of aberrant splicing events and cryptic promoters by testing the integrity of the p27 IRES^{T} mRNA (Supplementary Fig. S1). Using p27 IRES^{T} mice, we detected robust p27 IRES-mediated translation in the pituitary gland whereas other tissues showed either low or absent activity (Fig. 1B).

Thus, p27 expression in the pituitary is controlled at least in part by IRES-mediated translation. We therefore focused our attention on the pituitary gland, where p27 IRES-dependent translation is active and asked whether this activity might be impaired in DKC1^{m} mice. We observed a strong reduction in p27 IRES-dependent activity within the pituitary of DKC1^{m} animals (Fig. 1C). No differences were observed in cap-dependent translation, which is consistent with our previous results (10). These findings suggest that IRES-dependent translation of p27 protein is active within the pituitary, reflecting a cap-independent translation mechanism that might be required to maintain accurate protein levels in more differentiated and quiescent cells.

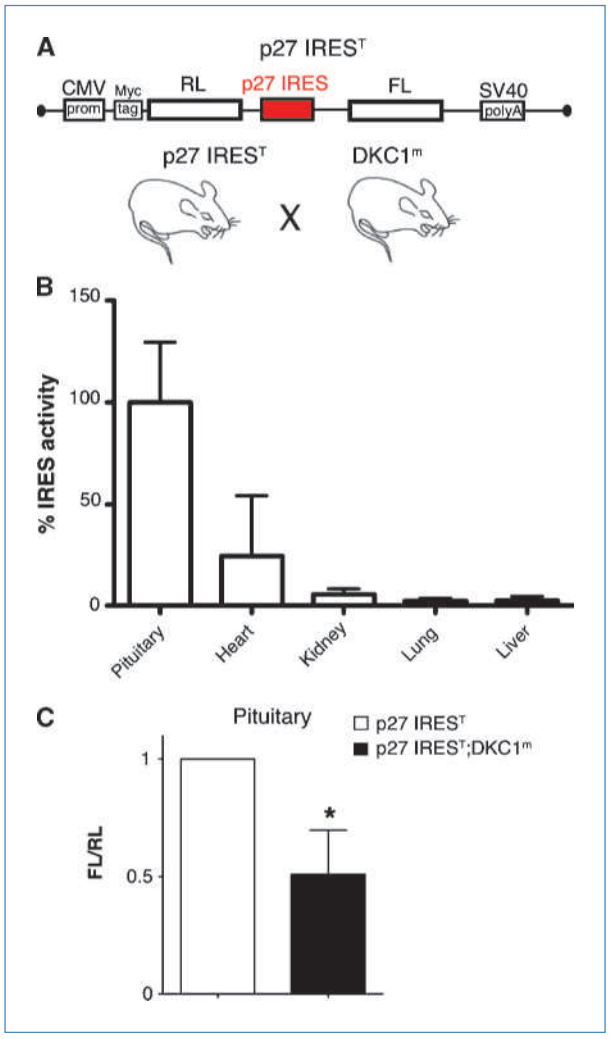

Figure 1. Analysis of p27 IRES-mediated translation using a new bioluminescent mouse model reveals robust translational control in the pituitary, which is reduced in the DKC1^{m} background. A, schematic of the dicistronic transgene used to generate bioluminescent p27 IRES^{T} animals. B, analysis of p27 IRES^{T} mice. Columns, mean percentage of p27 IRES activity (FLuc values) measured in different organs prepared from three p27 IRES^{T} mice and normalized by the mRNA dicistronic expression; bars, SEM. C, p27 IRES-mediated translation is markedly reduced in DKC1^{m} pituitary glands. Levels of p27 IRES-mediated translation were measured in pituitary glands isolated from p27 IRES^{T} and p27 IRES^{T};DKC1^{m} mice. Columns, mean ratio of FLuc/RLuc (FL/RL) measured in four pairs of age-matched animals; bars, SEM. Statistical analysis was carried out using Student's *t* test (*, $P < 0.05$).

Defining the molecular impairment in p27 IRES-dependent translation in DKC1^{m} cells

The molecular mechanisms by which defects in IRES-dependent translation occur when rRNA modifications are decreased in DKC1^{m} cells remain unknown. One outstanding question is whether this molecular impairment occurs at the stage of ribosome binding to specific mRNAs, as in the case of p27. To answer this question, we reconstituted the formation of an initiation complex of translation on the p27 IRES element, using WT and DKC1^{m} cytoplasmic extracts following serum starvation, a condition that strongly induces p27 IRES-mediated translation (10). This enabled us to investigate whether DKC1^{m} cells are impaired in the assembly of the preinitiation complex (48S), one of the most critical and earliest events in the translation initiation process in which interactions between mRNA-40S subunits occur (Fig. 2A; ref. 27). By analyzing the efficiency of the 48S complex formations in WT and DKC1^{m} cells, we found that the total amount of p27 IRES-containing preinitiation complexes is markedly reduced in DKC1^{m} compared with WT cells (Fig. 2B). These data indicate that rRNA modifications directly impinge on the assembly of a preinitiation complex of translation that mediates p27 IRES-dependent translation.

DKC1 and p27 genetically interact in pituitary tumorigenesis

The most prominent spontaneous tumor present in p27$^{-/-}$ mice is pituitary cancer of the intermediate lobe, which occurs after 3 months of age (18). As we observed robust

p27 IRES-dependent translation in the pituitary, we reasoned that reduced p27 translation in DKC1^{m} mice might cooperate in pituitary tumorigenesis. We therefore tested for a genetic interaction between *DKC1* and *p27*. Strikingly, histological analysis revealed pronounced hyperplasia of the intermediate lobe (pars intermedia) of p27$^{+/-}$;DKC1^{m} pituitary glands, which was already evident as early as 8 months of age, whereas no abnormalities are present in WT, p27$^{+/-}$, and DKC1^{m} mice at this age (Fig. 3A). These findings indicate that reductions in DKC1 expression significantly accelerate the onset of intermediate lobe hyperplasia in p27$^{+/-}$;DKC1^{m}. We next asked whether cooperation between *DKC1* and *p27* would progress and culminate in full-blown pituitary adenoma in p27$^{+/-}$;DKC1^{m} animals. By 15 months of age, p27$^{+/-}$;DKC1^{m} mice show a more dramatic intermediate lobe hyperplasia as well as pituitary adenomas (Fig. 3B). Indeed, histopathologic analysis of these tumors revealed the presence of numerous perivascular pseudorosette formations, typical features of primitive neuroectodermal carcinomas (Fig. 3B). Only a mild hyperplasia is present in p27$^{+/-}$ mice and DKC1^{m} mice at this stage (Fig. 3B). Taken together, these data suggest that p27 IRES-dependent translation may be a functionally important mechanism for tumor suppression within the pituitary.

A novel mutation in the *DKC1* gene is associated with a human pituitary tumor

We extended our analysis of DKC1 in human pituitary tumors. To date, cancer-associated mutations in *DKC1* have not been identified. We performed direct bidirectional sequencing of DNA isolated from 35 primary human pituitary adenomas. In this context, we identified a novel mutation of the *DKC1* gene in a tumor biopsy from a 61-year-old female patient diagnosed with nonfunctioning pituitary adenoma without previous history of disease. Histological analysis of the tumor showed negative staining for luteinizing hormone, follicle-stimulating hormone, thyroid-stimulating hormone, prolactin, adrenocorticotrophic hormone, and growth hormone. Magnetic resonance imaging revealed an intrasellar tumor with suprasellar extension and maximum diameters of 26, 24, and 20 mm in the vertical, horizontal, and anteroposterior axes, respectively. The tumor was infiltrating the sellar floor but not the dura mater and was surgically removed. However, the patient relapsed within 3 years from

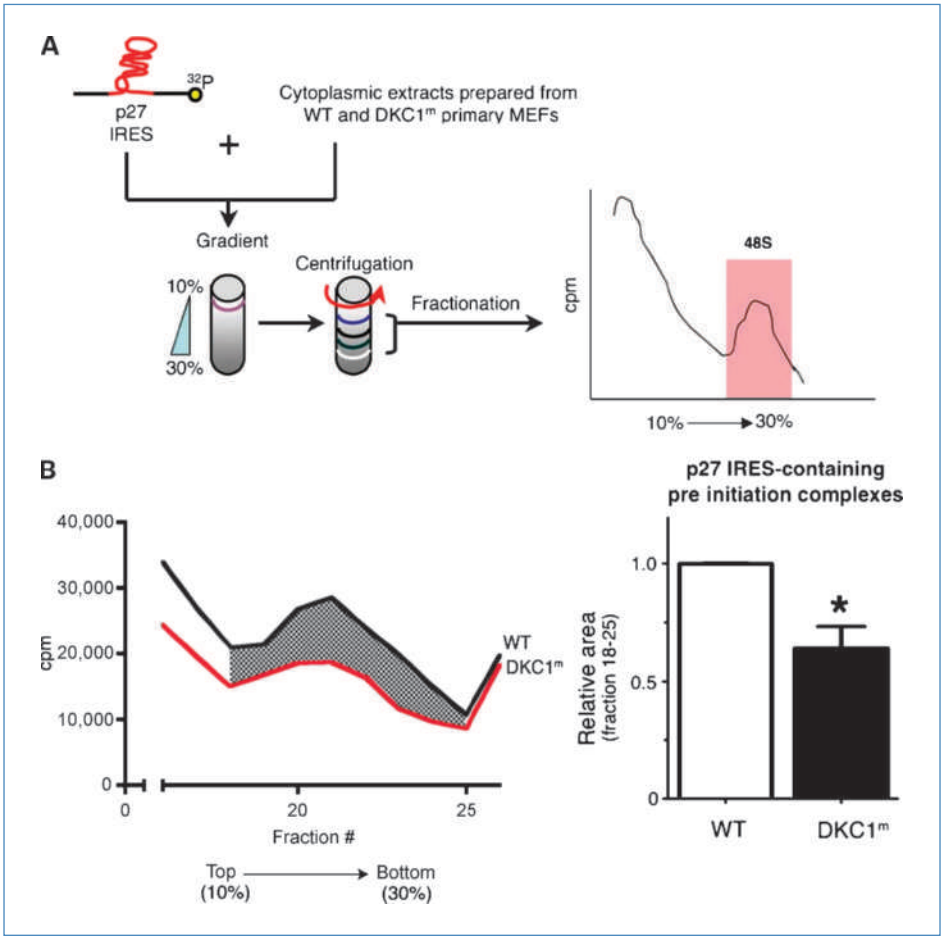

Figure 2. Molecular mechanism of p27 IRES-mediated translation impairment in DKC1^{m} cells. A, schematic of the biochemical approach used to study the 48S complex formation in WT and DKC1^{m} MEFs. A [^{32}P]p27 IRES mRNA probe was incubated with cytoplasmic extracts. Newly assembled 48S complexes were separated by sucrose gradient centrifugation and fractionated according to their density. A peak of radioactivity was generated and coincided with fractions containing the 48S complexes. B, representative of the 48S subunit quantification from total cytoplasmic extracts prepared from serum-starved (0.1% fetal bovine serum) WT and DKC1^{m} cells. Representative profile of a sucrose density gradient reporting the radioactive intensity per fraction in WT (black) and DKC1^{m} (red) extracts, respectively (left). Columns, mean of the area under the curve in WT and DKC1^{m} cell extracts measured in three independent experiments; bars, SEM (right). Statistical analysis was carried out using Student's *t* test (*, $P < 0.05$).

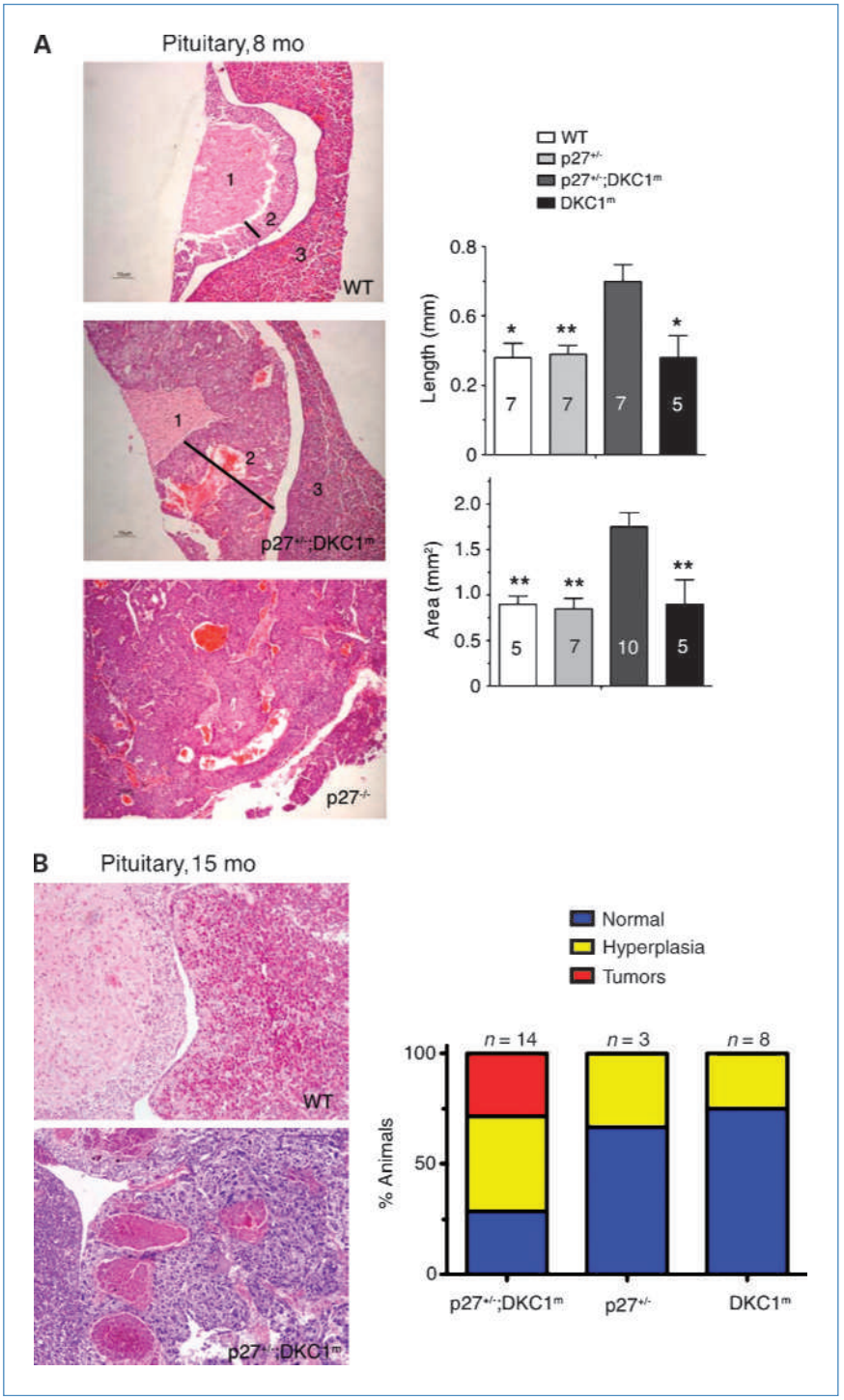

Figure 3. DKC1 and p27 genetically cooperate toward pituitary tumorigenesis. A, micrographs of H&E-stained paraffin sections prepared from pituitary glands of 8-mo-old WT, $p27^{+/-}$;$DKC1^{m}$ (hyperplasia) and $p27^{-/-}$ (tumor) animals. Numbers on the pictures indicate: (1) pars nervosa, (2) pars intermedia (intermediate lobe), and (3) pars distalis, bars, 10 nm. Columns, mean length and area of the intermediate lobe; bars, SEM. The number of animals analyzed for each genotype is indicated on the columns. Statistical analysis was performed using unpaired two-tailed *t* tests (**, $P < 0.01$; *, $P < 0.05$). B, representative histopathologic analysis of a normal pituitary gland (top) and a pituitary carcinoma (bottom) from 15-mo-old WT and $p27^{+/-}$;$DKC1^{m}$ mice, respectively. Graph shows the percentages of double $p27^{+/-}$;$DKC1^{m}$, $p27^{+/-}$ and $DKC1^{m}$ animals with a normal pituitary (blue), pituitary hyperplasia (yellow), and pituitary cancers (red).

the initial surgery and radiosurgery was necessary to remove a pathologic growth of intrasellar tissue adjacent to the right cavernous sinus. Sequencing analysis of DNA isolated from the primary tumor showed a point mutation in one copy of the X-linked *DKC1* gene, which corresponded with a novel A to G nucleotide variation located in exon 14. This results in a nonsynonymous serine (S) to glycine (G) substitution at position 485 (henceforth referred to as $DKC1^{S485G}$) in the COOH-terminal portion of the protein (Fig. 4A). This point mutation in *DKC1* has not been previously reported in dyskeratosis congenita. Therefore, we next sought to determine whether and how the $DKC1^{S485G}$ alters dyskerin protein

expression and/or activity. We engineered the *DKC1*^{S485G} mutation in an exogenous copy of *DKC1* and found that it was significantly less stable than the DKC1 protein (Fig. 4B). Consistent with these findings, we observed that in the DKC1^{S485G} primary tumor sample, DKC1 protein levels were significantly reduced but not affected at the mRNA level (Fig. 4C). Decreases in DKC1 activity were also evident as we observed a reduction in 18S rRNA pseudouridylation levels (Fig. 5A). Importantly, it has been previously shown that *DKC1* mutations affect the accumulation of telomerase RNA (TERC) and alter telomerase complex activity (28). Therefore, we measured TERC RNA levels in the DKC1^{S485G} mutant tumor (Fig. 5B). We did not find any significant reduction of TERC RNA levels in the DKC1^{S485G} mutant tumor when compared with normal pituitary tissues (Fig. 5B), which suggests that this specific *DKC1* mutation might not affect telomerase activity.

Next, we analyzed p27 levels in the primary tumor sample that harbored the DKC1^{S485G} mutation. Consistent with our results showing the importance of dyskerin in p27 translational control, we found that p27 protein expression was significantly diminished whereas p27 mRNA expression was comparable to normal pituitary tissue (Fig. 5C).

Discussion

In this study, we used a novel genetic reporter system to monitor a specific mode of p27 translation control that occurs via an IRES element positioned in the 5′-untranslated

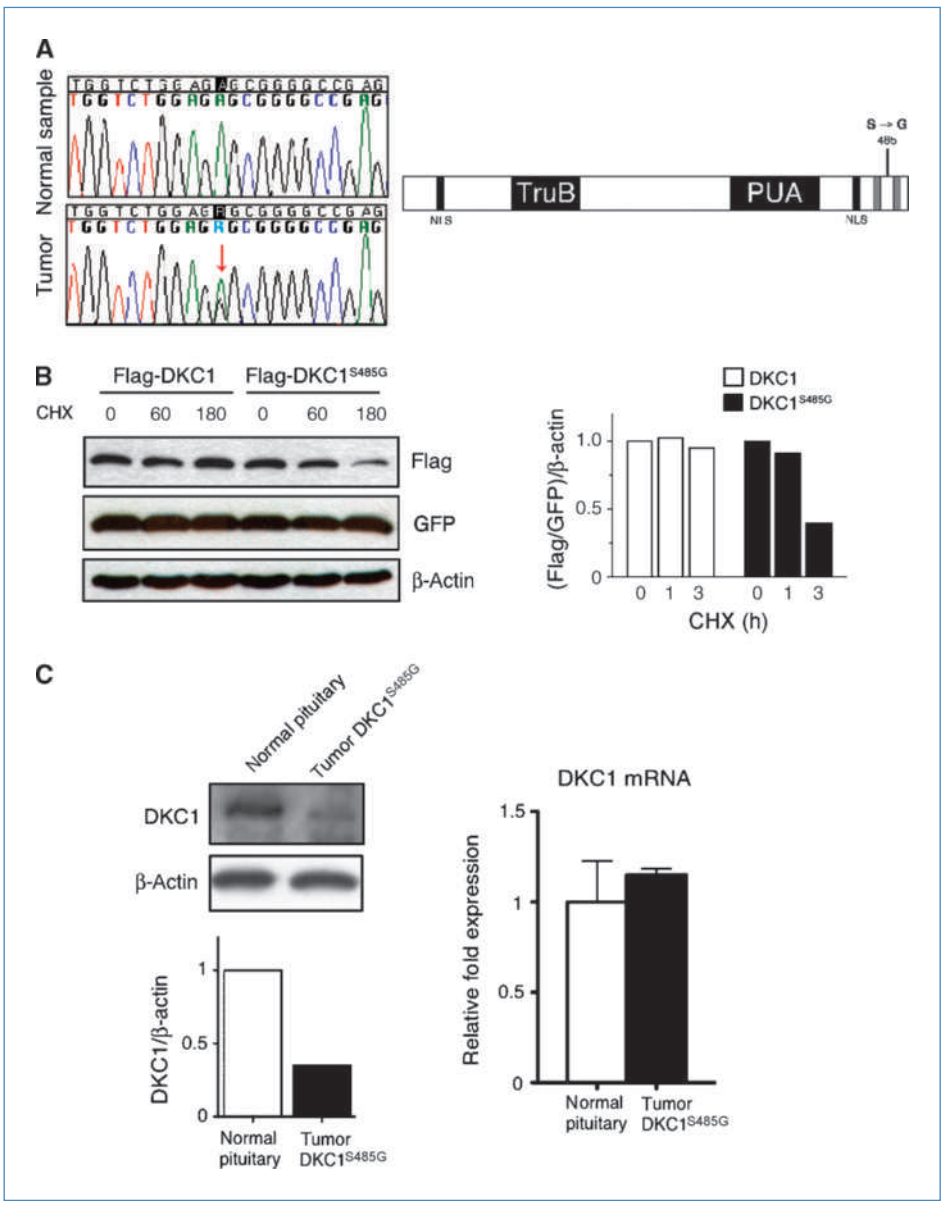

Figure 4. Identification of a novel DKC1 mutation in a human pituitary adenoma. A, chromatographs showing a novel mutation in the DKC1 locus identified in a human pituitary adenoma (left). Scheme of the mutation, an A1493G variation located on one *DKC1* allele leads to the amino acid change S485G in the COOH-terminal portion of the protein (right). B, analysis of DKC1^{S485G} protein stability. Densitometric analysis of the DKC1 levels was done at each time point after blockage of protein synthesis as indicated. GFP was cotransfected for transfection efficiency and β-actin was used as loading control. C, DKC1 protein (left) and mRNA (right) levels in a normal pituitary and in the tumor bearing the mutation DKC1^{S485G}. Densitometric analysis of DKC1 over β-actin protein levels in each sample (bottom left).

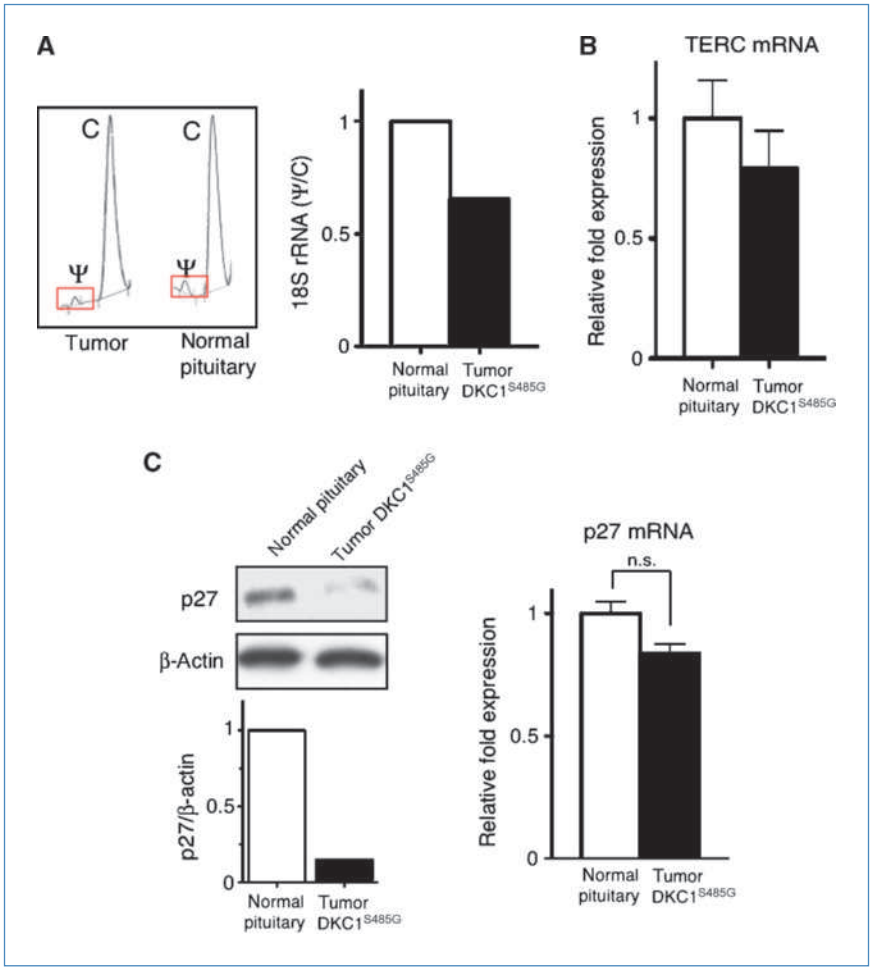

Figure 5. Impaired rRNA pseudouridylation is associated with reductions of p27 protein levels but not of the telomerase RNA component (TERC) in the DKC1^{S485G} mutant tumor. A, chromatographs of high-performance liquid chromatography analysis of the 18S rRNA pseudouridylation. Bar graph shows quantification of the ψ/C ratio in samples from normal pituitary and the DKC1^{S485G} mutant tumor. B, the levels of TERC were measured by quantitative PCR in two normal pituitaries and the DKC1^{S485G} pituitary tumor. Analysis was performed in triplicate on two different samples per specimen. No significant differences between the samples were found. $P > 0.05$ was determined using the unpaired two-tailed *t* test. C, p27 protein levels are markedly reduced in the tumor carrying the DKC1^{S485G} mutation. Western blot (left) and quantitative PCR analysis (right) of p27 expression were performed using protein extracts and total RNA prepared from a normal pituitary and the tumor carrying the DKC1^{S485G} mutation. Densitometric analysis of p27 over β-actin levels is shown (bottom left). No significant differences in p27 mRNA levels were measured between the samples. $P > 0.05$ was determined by employing the unpaired two-tailed *t* test.

region of the p27 mRNA. We observed robust control of p27 IRES-dependent translation in the pituitary and found that this activity was severely impaired in hypomorphic DKC1^{m} mice. At the molecular level, we showed that DKC1^{m} ribosomes had a defect in 48S preinitiation complex formation on the p27 IRES element. We functionally extend these findings by identifying a genetic interaction between DKC1^{m} and p27$^{+/-}$ mice leading to the formation of pituitary tumors. The cooperation of other distinct oncogenic lesions has been studied using compound mice to elucidate the molecular mechanisms underlying pituitary tumor development (11). For example, compound Rb$^{+/-}$;Pttg$^{-/-}$ and Rb$^{+/-}$;Skp2$^{-/-}$ mice show a reduced frequency of pituitary tumors (29, 30). In contrast, genetic loss of *p21* gene contributes to accelerated pituitary tumor formation in Rb heterozygous mice, and similarly, mice lacking both *p27* and *p18* rapidly develop lethal pituitary adenomas (31, 32).

Importantly, our results led us to undertake direct sequencing of the *DKC1* gene in primary human pituitary tumors, which identified a novel mutation in DKC1. The *DKC1^{S485G}* mutation leads to a decrease in dyskerin protein stability and activity, and is associated with decreases in rRNA modifications and p27 protein levels.

Furthermore, it would be important to study whether, beside point mutations, additional epigenetic events might deregulate DKC1 expression in pituitary adenomas. In this regard, several studies indicate that hypermethylation of specific CpG islands located within promoter regions of genes encoding for tumor suppressors such as Rb, GADD45γ, p16, maternal express gene-3, and pituitary tumor apoptosis gene is associated with loss of protein expression in a number of pituitary tumors (33, 34).

The multiple endocrine neoplasia type 1 (*MEN1*) gene is mutated in the eponymous syndrome, which is characterized by increased predisposition to pituitary adenoma formation (35). Interestingly, a germ line point mutation in the *p27* gene has been identified in a MEN1 patient harboring no mutation in *MEN1* gene and presenting with pituitary tumors (36). However, decreased p27 expression has been reported in many human cancers without mutations in the gene (17). Therefore, reductions in p27 expression, by alterations in pathways that control p27 expression, might contribute to the initiation or progression of cancer. It is tempting to

speculate that alterations in p27 mRNA translation might represent an early event in clonal expansion leading to the pituitary adenoma phenotype. In support of this hypothesis, ubiquitin-mediated degradation of p27 controlled by SKP2 does not seem to correlate with a reduction in p27 protein expression in pituitary tumors (19). At the molecular level, we show that impairments in rRNA modifications directly affect a very early step in p27-IRES translation initiation. Interestingly, defects in a second type of rRNA modification, rRNA methylation, have been implicated in tumorigenesis (37, 38). For example, loss of the *U50* gene that mediates rRNA methylation has been linked to the pathogenesis of human breast and prostate cancers (39, 40). Therefore, deregulations of rRNA modifications might have broad implications for tumors arising from somatic mutations in ribosome components. Our study sets the rationale for screening for additional somatic *DKC1* mutations in human tumors.

Disclosure of Potential Conflicts of Interest

No potential conflicts of interest were disclosed.

Acknowledgments

We thank Dr. Barna for critical discussion and reading of the manuscript, Lynn Delos Santos and Anthony Karnezis for technical support, and Olivia F. Siegel for editing the manuscript.

Grant Support

R01 HL085572 (D. Ruggero) and 3R01HL085572-05S1 (D. Ruggero).

The costs of publication of this article were defrayed in part by the payment of page charges. This article must therefore be hereby marked *advertisement* in accordance with 18 U.S.C. Section 1734 solely to indicate this fact.

Received 01/04/2010; revised 04/14/2010; accepted 05/03/2010; published OnlineFirst 06/29/2010.

References

1. Kirwan M, Dokal I. Dyskeratosis congenita: a genetic disorder of many faces. Clin Genet 2008;73:103–12.
2. Montanaro L, Brigotti M, Clohessy J, et al. Dyskerin expression influences the level of ribosomal RNA pseudo-uridylation and telomerase RNA component in human breast cancer. J Pathol 2006;210:10–8.
3. Sieron P, Hader C, Hatina J, et al. DKC1 overexpression associated with prostate cancer progression. Br J Cancer 2009;101:1410–6.
4. Poncet D, Belleville A, t'kint de Roodenbeke C, et al. Changes in the expression of telomere maintenance genes suggest global telomere dysfunction in B-chronic lymphocytic leukemia. Blood 2008;111:2388–91.
5. Meier UT. The many facets of H/ACA ribonucleoproteins. Chromosoma 2005;114:1–14.
6. Ruggero D, Grisendi S, Piazza F, et al. Dyskeratosis congenita and cancer in mice deficient in ribosomal RNA modification. Science 2003;299:259–62.
7. Holcik M, Sonenberg N. Translational control in stress and apoptosis. Nat Rev Mol Cell Biol 2005;6:318–27.
8. Silvera D, Arju R, Darvishian F, et al. Essential role for eIF4GI overexpression in the pathogenesis of inflammatory breast cancer. Nat Cell Biol 2009;11:903–8.
9. Barna M, Pusic A, Zollo O, et al. Suppression of Myc oncogenic activity by ribosomal protein haploinsufficiency. Nature 2008;456:971–5.
10. Yoon A, Peng G, Brandenburger Y, et al. Impaired control of IRES-mediated translation in X-linked dyskeratosis congenita. Science 2006;312:902–6.
11. Melmed S. Acromegaly pathogenesis and treatment. J Clin Invest 2009;119:3189–202.
12. Nikitin A, Lee WH. Early loss of the retinoblastoma gene is associated with impaired growth inhibitory innervation during melanotroph carcinogenesis in $Rb^{+/-}$ mice. Genes Dev 1996;10:1870–9.
13. Lee EY, Chang CY, Hu N, et al. Mice deficient for Rb are nonviable and show defects in neurogenesis and haematopoiesis. Nature 1992;359:288–94.
14. Pei L, Melmed S, Scheithauer B, Kovacs K, Benedict WF, Prager D. Frequent loss of heterozygosity at the retinoblastoma susceptibility gene (RB) locus in aggressive pituitary tumors: evidence for a chromosome 13 tumor suppressor gene other than RB. Cancer Res 1995;55:1613–6.
15. Pei L, Melmed S. Isolation and characterization of a pituitary tumor-transforming gene (PTTG). Mol Endocrinol 1997;11:433–41.
16. Abbud RA, Takumi I, Barker EM, et al. Early multipotential pituitary focal hyperplasia in the α-subunit of glycoprotein hormone-driven pituitary tumor-transforming gene transgenic mice. Mol Endocrinol 2005;19:1383–91.
17. Slingerland J, Pagano M. Regulation of the cdk inhibitor p27 and its deregulation in cancer. J Cell Physiol 2000;183:10–7.
18. Fero ML, Randel E, Gurley KE, Roberts JM, Kemp CJ. The murine gene p27Kip1 is haplo-insufficient for tumour suppression. Nature 1998;396:177–80.
19. Musat M, Korbonits M, Pyle M, et al. The expression of the F-box protein Skp2 is negatively associated with p27 expression in human pituitary tumors. Pituitary 2002;5:235–42.
20. Millard SS, Yan JS, Nguyen H, Pagano M, Kiyokawa H, Koff A. Enhanced ribosomal association of p27(Kip1) mRNA is a mechanism contributing to accumulation during growth arrest. J Biol Chem 1997;272:7093–8.
21. Hengst L, Reed SI. Translational control of p27Kip1 accumulation during the cell cycle. Science 1996;271:1861–4.
22. Chu IM, Hengst L, Slingerland JM. The Cdk inhibitor p27 in human cancer: prognostic potential and relevance to anticancer therapy. Nat Rev Cancer 2008;8:253–67.
23. Gopfert U, Kullmann M, Hengst L. Cell cycle-dependent translation of p27 involves a responsive element in its 5′-UTR that overlaps with a uORF. Hum Mol Genet 2003;12:1767–79.
24. Miskimins WK, Wang G, Hawkinson M, Miskimins R. Control of cyclin-dependent kinase inhibitor p27 expression by cap-independent translation. Mol Cell Biol 2001;21:4960–7.
25. Kullmann M, Gopfert U, Siewe B, Hengst L. ELAV/Hu proteins inhibit p27 translation via an IRES element in the p27 5′UTR. Genes Dev 2002;16:3087–99.
26. Costa-Mattioli M, Svitkin Y, Sonenberg N. La autoantigen is necessary for optimal function of the poliovirus and hepatitis C virus internal ribosome entry site *in vivo* and *in vitro*. Mol Cell Biol 2004;24:6861–70.
27. Sonenberg N, Hinnebusch AG. Regulation of translation initiation in eukaryotes: mechanisms and biological targets. Cell 2009;136:731–45.
28. Mochizuki Y, He J, Kulkarni S, Bessler M, Mason PJ. Mouse dyskerin mutations affect accumulation of telomerase RNA and small nucleolar RNA, telomerase activity, and ribosomal RNA processing. Proc Natl Acad Sci U S A 2004;101:10756–61.
29. Chesnokova V, Kovacs K, Castro AV, Zonis S, Melmed S. Pituitary hypoplasia in $Pttg^{-/-}$ mice is protective for $Rb^{+/-}$ pituitary tumorigenesis. Mol Endocrinol 2005;19:2371–9.
30. Wang H, Bauzon F, Ji P, et al. Skp2 is required for survival of aberrantly proliferating Rb1-deficient cells and for tumorigenesis in $Rb1^{+/-}$ mice. Nat Genet 42:83–8.

31. Chesnokova V, Zonis S, Kovacs K, et al. p21(Cip1) restrains pituitary tumor growth. Proc Natl Acad Sci U S A 2008;105:17498–503.
32. Franklin DS, Godfrey VL, Lee H, et al. CDK inhibitors p18(INK4c) and p27(Kip1) mediate two separate pathways to collaboratively suppress pituitary tumorigenesis. Genes Dev 1998;12:2899–911.
33. Simpson DJ, Hibberts NA, McNicol AM, Clayton RN, Farrell WE. Loss of pRb expression in pituitary adenomas is associated with methylation of the RB1 CpG island. Cancer Res 2000;60:1211–6.
34. Farrell WE. Pituitary tumours: findings from whole genome analyses. Endocr Relat Cancer 2006;13:707–16.
35. Marx SJ, Agarwal SK, Kester MB, et al. Multiple endocrine neoplasia type 1: clinical and genetic features of the hereditary endocrine neoplasias. Recent Prog Horm Res 1999;54:397–438, discussion-9.
36. Pellegata NS, Quintanilla-Martinez L, Siggelkow H, et al. Germ-line mutations in p27Kip1 cause a multiple endocrine neoplasia syndrome in rats and humans. Proc Natl Acad Sci U S A 2006; 103:15558–63.
37. Belin S, Beghin A, Solano-Gonzalez E, et al. Dysregulation of ribosome biogenesis and translational capacity is associated with tumor progression of human breast cancer cells. PLoS One 2009;4:e7147.
38. Munholland JM, Nazar RN. Methylation of ribosomal RNA as a possible factor in cell differentiation. Cancer Res 1987;47:169–72.
39. Dong XY, Guo P, Boyd J, et al. Implication of snoRNA U50 in human breast cancer. J Genet Genomics 2009;36:447–54.
40. Dong XY, Rodriguez C, Guo P, et al. SnoRNA U50 is a candidate tumor-suppressor gene at 6q14.3 with a mutation associated with clinically significant prostate cancer. Hum Mol Genet 2008;17: 1031–42.